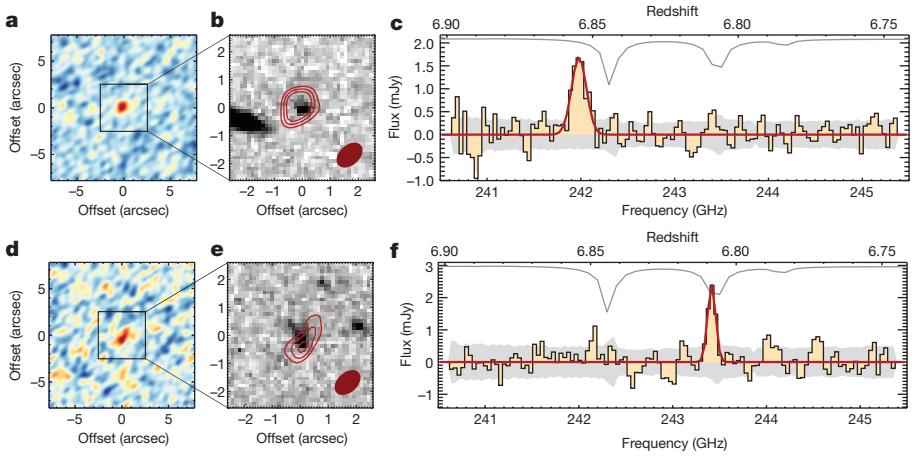

Figure 1 | Spectroscopic line confirmations of the galaxies targeted in this study. ALMA line maps and spectra for two galaxies with photometric redshifts (z_{phot}) in the range $6.6 < z_{phot} < 6.9$ (ref. 7). We detect a 8.2σ [C II] line at $z_{[C\,II]} = 6.8540 \pm 0.0003$ in galaxy COS-3018555981 (**a**–**c**), and a roughly 5.1σ [C II] line at $z_{[C\,II]} = 6.8076 \pm 0.0002$ in galaxy COS-2987030247 (**d**–**f**). **a**, **d**, $20'' \times 20''$ images of the ALMA cube (before primary-beam correction), collapsed over 241.85–242.10 GHz for COS-3018555981 and 243.35–243.45 GHz for COS-2987030247 (with root-mean-squares of 0.1 mJy and 0.2 mJy, respectively). **b**, **e**, $5'' \times 5''$ images of the targeted sources. Hubble Space Telescope H_{160}-band imaging is shown in greyscale; the overlaid red contours show the 3σ, 4σ and 5σ levels of the spectral-line-averaged maps on the left. The filled ellipses in the bottom right corners indicate the beam size ($1.1'' \times 0.7''$ half-power widths). **c**, **f**, The spectra extracted from within a contour of the half-maximum power in the line maps. The red lines show the best-fitting Gaussian line profiles; the grey lines at the top show the atmospheric absorption; the grey filled regions give the $\pm 1\sigma$ noise in the spectrum.

that these galaxies fall substantially below the local relation[1–5]. This is probably because we chose our $z > 6.5$ targets differently to previous authors: we selected [O III] + Hβ emitters as opposed to Lyman-α-emitting galaxies.

Our sources have slightly higher SFRs and redder UV slopes (at roughly −1.2) than previously studied galaxies from this epoch, which could indicate that our galaxies are more evolved and more metal rich. Sources with extremely low oxygen abundance in the local Universe are typically found to be [C II] deficient[15,18] owing to their hard radiation field, and therefore metallicity could be an important discriminator between [C II]-bright and [C II]-faint sources[19]. Moreover, in local galaxies the SFR surface density (Σ_{SFR}) drives a continuous trend of deepening [C II] deficit as a function of increasing Σ_{SFR} (refs 18, 20), indicating that local processes such as the radiation-field intensity are important in driving [C II] luminosity. If [C II]-faint sources at $z > 6$, currently unresolved in [C II] lines, have higher star-formation surface brightness than our galaxies, this could also explain the different SFR/$L_{[C\,II]}$ ratios.

Furthermore, our sources have high-equivalent-width optical emission lines, which could suggest an ongoing starburst and potentially a higher fraction of [C II] emission emerging from H II regions. Starbursts and H II galaxies in the local Universe have slightly elevated [C II] luminosities for a given SFR[15], and therefore we could specifically be targeting the brightest [C II] galaxies of the overall $z \approx 7$ galaxy population. Finally, while we do not have spectroscopy covering the Lyman-α line for COS-3018555981 and COS-2987030247, our sources could be weaker Lyman-α emitters than are typically seen in spectroscopically confirmed sources at this redshift. Lyman-α emission is suggested to be inversely correlated with neutral gas column density[21] and can therefore affect the visibility of [C II], which emerges both in the diffuse neutral and in the warm ionized medium of a galaxy.

We also determined [C II] half-light radii (deconvolved from the beam size) of 2.6 ± 0.8 kpc and 3.1 ± 1.0 kpc for COS-3018555981 and COS-2987030247—nearly twice the half-light radius of the UV in the brightest LBGs at this redshift[22]. We used the spatial extent of the [C II] detection to investigate the velocity structure of these sources, which reveals a projected velocity difference over the galaxy of 111 ± 28 km s^{-1} and 54 ± 20 km s^{-1} for COS-3018555981 and COS-2987030247, respectively (Fig. 3), similar to the velocity gradients observed recently in two galaxies at redshifts of around 5–6 (refs 23, 24). Given the low angular resolution of the observations, there are various ways to interpret these velocity gradients. A rotating galaxy disk would be one interpretation; however, a merger involving one or more [C II]-emitting galaxies, smoothed by the beam size, could also appear as a regular rotational field. Furthermore, a bipolar outflow or perhaps an inflow of gas could provide an additional velocity component to the [C II] line that might give the impression of galaxy rotation.

We applied an observational criterion for the classification of rotation- and dispersion-dominated systems, based on the full observed velocity gradient, Δv_{obs}, and the integrated line width, σ_{tot}, of a galaxy, such that $\Delta v_{obs}/2\sigma_{tot}$ values of more than 0.4 are likely to be rotation-dominated sources[25]. In Fig. 4, we compare this quantity for

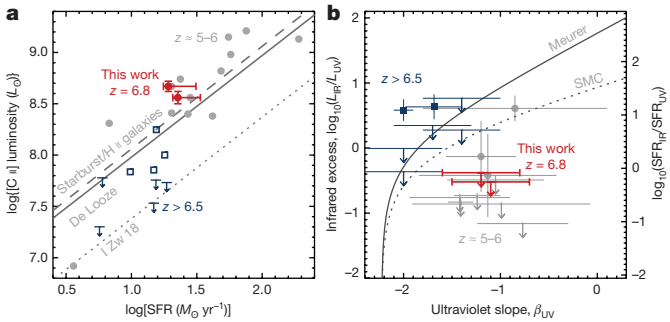

Figure 2 | [C II] luminosity and dust continuum for $z > 5$ galaxies. **a**, [C II] line luminosity as a function of the SFR for COS-3018555981 and COS-2987030247 (red points; error bars for the SFRs reflect 1σ upper limits on the infrared continuum), compared with [C II] detections at redshifts of around 5–6 (light grey points)[4,16,17] and more than 6.5 (blue open squares and arrows)[1–3,5]. Locally observed relations[15] are indicated by solid lines (star-forming galaxies) and dashed lines (starburst and H II galaxies). The dotted line gives the 0.6-dex offset from the local relation found for the dwarf galaxy I Zwicky 18 ('I Zw 18'). **b**, Infrared excess (L_{UV}/L_{IR}) as a function of the UV-continuum slope (β_{UV}) of our sources compared with expectations from the Meurer[13] relation (solid grey line) and a similar relation based on the dust law of the Small Magellanic Cloud[14] (SMC; dotted grey line). We include [C II] detections at redshifts of around 5–6 as light grey points[16], and detections (and upper limits) at redshifts greater than 6.5 as blue solid squares (and arrows)[28–30]. Upper limits and error bars represent 1σ significance levels. $L_{\odot}$, luminosity of the Sun.